IOP FTC

IOP PUBLISHING JOURNAL OF PHYSICS: CONDENSED MATTER

J. Phys.: Condens. Matter **19** (2007) 472202 (10pp) doi:10.1088/0953-8984/19/47/472202

FAST TRACK COMMUNICATION

Mechanism of ultraviolet photoconductivity in zinc oxide nanoneedles

Sanjeev Kumar[1,2], Gil-Ho Kim[1], K Sreenivas[2] and R P Tandon[2]

[1] School of Information and Communication Engineering, and SKKU Advanced Institute of Nanotechnology, Sungkyunkwan University, Suwon 440-746, Korea
[2] Department of Physics and Astrophysics, University of Delhi, Delhi-110007, India

E-mail: sanjeev@skku.edu and ghkim@skku.edu

Received 24 August 2007, in final form 16 October 2007
Published 5 November 2007
Online at stacks.iop.org/JPhysCM/19/472202

Abstract

Ultraviolet photoconductivity in zinc oxide (ZnO) nanoneedles grown on the surface of a multilayer structure comprised of ZnO film (50 nm)/Zn layer (20 nm)/ZnO film (2 μm) fabricated on a stainless steel substrate using an unbalanced magnetron sputtering technique is reported. It was observed that the multilayered structure with ZnO nanoneedles exhibited enhanced ultraviolet photoconductivity in comparison to the ZnO films that were without nanoneedles. The enhancement in the photoconductivity is attributed to the increase in the quantum yield of the photogenerated charge carriers due to the presence of nanoneedles. A successive slow photoresponse transient following after a fast rise is due to the establishment of equilibrium between the charge carriers in the conduction band and the trapping centers created due to the shallow defects in the ZnO film. The observed photoresponse is critically analyzed on the basis of trapping levels created by the oxygen species during the high pressure deposition of the ZnO multilayer. Results show the promise of ZnO nanostructures in ultraviolet detection applications.

1. Introduction

Interest in the science of nanomaterials has stimulated intensive research interest in the growth of nanostructures and the investigation of their properties. These one-dimensional nanostructured materials have shown novel properties which are entirely different from the bulk properties [1]. Nanostructures of wide band gap semiconductor materials are of particular interest for their optoelectronic properties. ZnO, a wide band gap semiconducting oxide, is a unique material with diverse properties and can be tailored for semiconducting, piezoelectric and optoelectronic applications. In recent years the richest family of nanostructures has been reported for ZnO amongst all other materials [2]. The nanostructures of ZnO include porous structures, nanowires, nanoneedles, nanorods, etc and have been synthesized by a variety of techniques including the chemical route method, thermal evaporation, vapor phase

transport, sol–gel, the laser ablation technique, chemical vapor deposition, and molecular beam epitaxy [3–9]. Large scale production of ZnO nanostructures is of interest in many commercial applications such as the design of large arrays of three-dimensional network of nanorods similar to the structures formed with highly oriented ferric oxide nanorod arrays that led to the development of a hematite wet photovoltaic cell [10].

The ultraviolet (UV) photoconductivity in ZnO has been under scrutiny for ultraviolet light detection applications [11–14]. The photoresponse behavior in ZnO has been shown to depend on the growth conditions, structural deformation, presence of defects, and the deposition technique [11–14]. Ultra thin films of ZnO grown by unbalanced magnetron sputtering have been shown to possess an enhanced UV responsivity in comparison to thick films [14]. The photoconductivity phenomena in ZnO is generally related to adsorption and desorption of the chemisorbed oxygen from the surface of ZnO. Upon illuminating with light having a wavelength larger than the band gap of the material, the photogenerated holes so produced will keep on desorbing the chemisorbed oxygen species, and the liberated electrons will result in an increase in photoconductivity. Such a mechanism can be effectively implemented if nanostructures of ZnO are grown, where the surface to volume ratio is larger in comparison to planar film structures. Few attempts have been made to study the photoresponse behavior of ZnO nanowires and nanorods. Kind *et al* [15] studied the photoresponse of ZnO nanowires grown by the vapor phase transport process, and explored their potential for optical switches. Keem *et al* [16] reported on the photoresponse behavior of ZnO nanowires grown by thermal evaporation of ZnO powder. They observed a slow rise in the photoconductivity due to the surface related process. Ahn *et al* [6] studied the photoconductivity of ZnO nanorods synthesized by the sol–gel technique and explained the response behavior on the basis of adsorption and desorption of water molecules on the surface of nanorods. However, no attempts have been made to enhance the photoconductivity of ZnO films by synthesizing ZnO nanostructures on their surfaces and especially by using the unbalanced magnetron sputtering technique, which is known to deposit ZnO films with enhanced ultraviolet photoconductivity [12].

In the present work, ZnO nanoneedles have been synthesized on the surface of a photoconducting ZnO film using the unbalanced magnetron sputtering technique. The ultraviolet photoconductivity is shown to be enhanced with the presence of ZnO nanoneedles and this is attributed to the increase in quantum yield of the photogenerated charge carriers due to the bulk related phenomena.

2. Experimental details

ZnO thin films and the ZnO nanostructures were prepared using an radio frequency (rf) magnetron sputtering technique. A six inch diameter metallic zinc (Zn) target (99.99% pure) was sputtered in the O_2:Ar gas ambient (80:20) under an applied rf power of 600 W. The magnetic configuration in the magnetron electrode was intentionally altered to provide an unbalanced magnetic field to accelerate the *in situ* ionic bombardment in the growing film to yield a porous microstructure [12]. The ZnO film (2.0 μm thick) was deposited on a stainless steel (SS) substrate at a relatively high sputtering pressure of around 30 mTorr. A higher pressure is known to create the native defects in the growing films and has a significant role in the photoconductivity phenomena [11, 12]. ZnO nanoneedles were grown on the surface of the ZnO film by using an ultra thin (20 nm) buffer layer of Zn. The Zn layer was deposited under similar processing conditions except in 100% Ar ambient. A 50 nm thin layer of ZnO was further sputtered on the Zn(20 nm)/ZnO(2 μm)/SS structure. The deposited multilayer structure was annealed in air at different temperatures (100, 200, 300, and 400 °C) for 1 h.

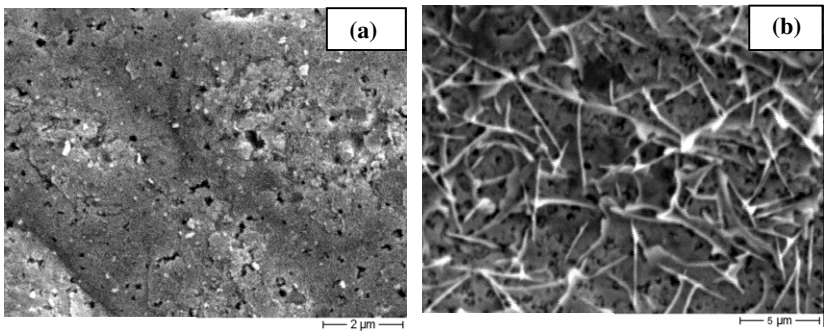

Figure 1. SEM images showing the growth of ZnO nanoneedles: (a) porous microstructure of ZnO film (2 μm thick) on an SS substrate, (b) ZnO nanoneedles on the surface of a ZnO multilayer annealed at 400 °C.

The surface morphology of the ZnO film and its nanostructures were studied using scanning electron microscopy (SEM). A Philips x-ray diffraction system was used to study the crystallographic orientation. Ultraviolet photoresponse relaxation studies were performed on the ZnO samples by evaporating aluminum planar electrodes separated by a distance of 2 mm. The photoresponse transients were measured at room temperature using a black ray UV lamp (model B 100 AP, $\lambda = 365$ nm), Keithley microvolt ammeter (model 150B), and a Tektronix digital storage oscilloscope (model TDS 3032B). A Newport optical power meter (model 1830-C) was used to measure the intensity of UV light.

3. Results and discussion

3.1. Growth of ZnO nanoneedles

ZnO film (2 μm thick) on a SS substrate was found to possess a preferred *c*-axis orientation. The surface roughness of the film was estimated to be very high (∼130 Å) and is attributed to the high pressure deposition of the film (30 mTorr). SEM analysis showed that the ZnO film on the SS substrate had a porous microstructure with the presence of large amount of voids (figure 1(a)). The presence of porosity could be attributed to deposition under relatively high O_2 partial pressure using an unbalanced magnetron electrode configuration. ZnO nanoneedles were observed on the surface of the multilayer structure when annealed at 300–400 °C. The details regarding the growth and the growth mechanism of the ZnO nanoneedles are reported elsewhere [13]. Figure 1(b) shows the SEM micrographs of the deposited layered structure ZnO(50 nm)/Zn(20 nm)/ZnO(2 μm)/SS annealed in air at 400 °C. Figure 2 shows the schematic diagram of the nanoneedle formation on the surface of the ZnO film. The ultrathin (20 nm) film of Zn is expected to be distributed with a discontinuous structure on the thick ZnO film (2 μm) surface and may act as a catalyst to seed the growth of ZnO nanoneedles when annealed at moderate temperature (300–400 °C). The catalytic driven growth of ZnO nanostructures using gold, silver, and graphite as seed has been reported by other workers as well using other techniques [8, 9, 17]. In a recent report [18], ZnO nanowires were synthesized by physical vapor deposition by evaporating Zn powder at 750 °C, and the nanowire growth was observed on a pulsed laser ablated ZnO thin film deposited on a Al_2O_3 substrate placed downstream of the furnace tube. They attributed the evaporated Zn particles with acting as a self catalyst and resulting in the growth of ZnO nanowires.

The XRD pattern of the ZnO nanoneedles grown on the ZnO surface showed peaks corresponding to ZnO powder only and revealed a polycrystalline structure, as shown in

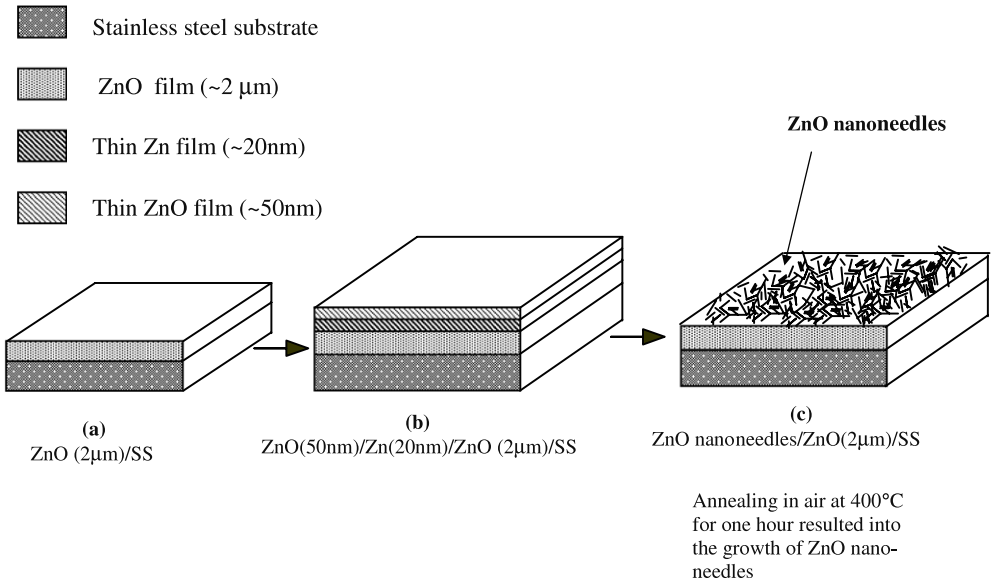

Figure 2. Schematic diagram showing the various steps involved in the growth of ZnO nanoneedles: (a) ZnO film (2 μm) deposited on an SS substrate, (b) ZnO multilayer comprised of ZnO (50 nm)/Zn(20 nm)/ZnO(2 μm)/SS, and (c) growth of ZnO nanoneedles on the surface of a ZnO film when the multilayer structure was annealed at 400 °C.

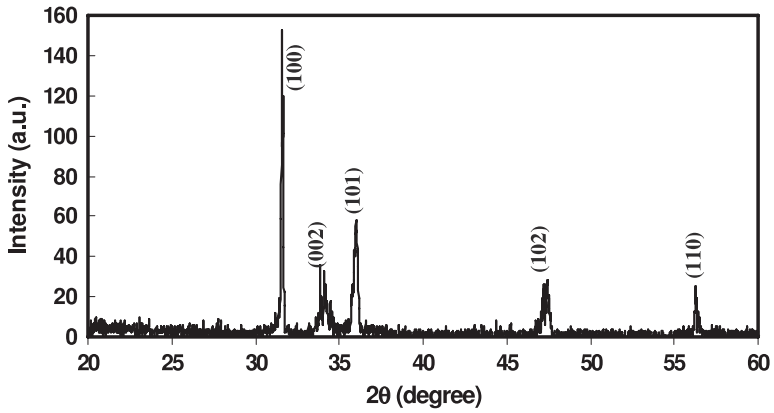

Figure 3. X-ray diffraction patterns of ZnO nanoneedles obtained on the surface of the ZnO film.

figure 3. It is important to point out that the underlying ZnO film (2.0 μm) in the multilayer structure was preferentially oriented with the *c*-axis normal to the substrate, whereas the nanoneedles formed on the surface are of mixed orientation and polycrystalline in nature. It is reported that the ZnO films possessing polycrystalline nature exhibit a higher photoconductivity in comparison to the preferentially oriented films [11, 12]. Therefore, we are expecting enhanced photoconductivity in ZnO films coated with ZnO nanoneedles. The two structures (A) ZnO film (2 μm)/SS and (B) ZnO nanoneedles/ZnO (2 μm)/SS as shown in figures 2(a) and (c) respectively were chosen for the ultraviolet photoconductivity study to reveal the influence of the dispersal of nanoneedles on the surface of ZnO in the observed photoconductivity transient.

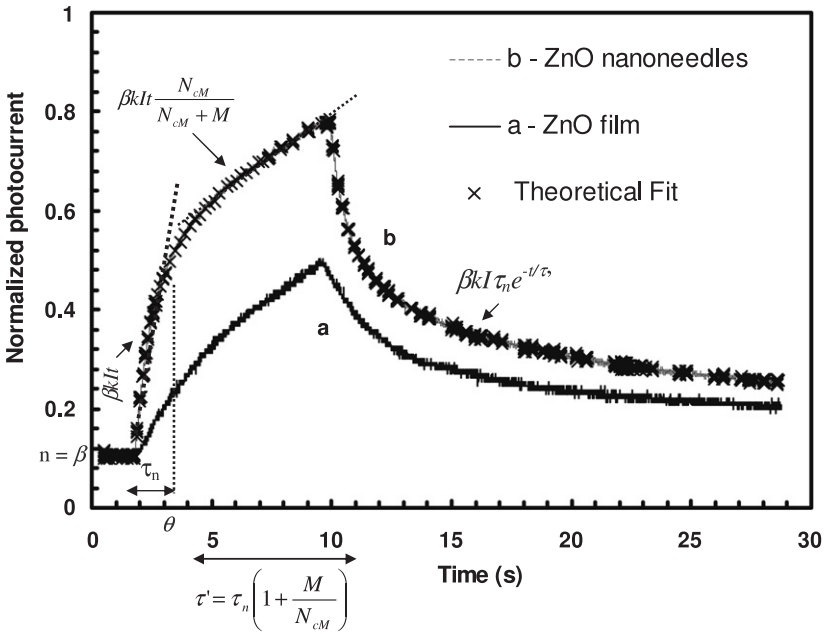

Figure 4. Photoresponse relaxation curves of: (a) ZnO film (2 μm) on an SS substrate, and (b) ZnO nanoneedles obtained on the surface of the ZnO film. The solid curve (b) represents the experimentally observed response and the marker (×) represents the theoretical fit of the photoresponse behavior of ZnO nanoneedles.

3.2. Ultraviolet photoresponse

Figure 4 shows the UV photoresponse transient on both the structures A and B at room temperature under a UV light illumination intensity of 1 mW cm^{-2}. The photoresponse transient of the structure A was found to increase with time slowly under UV illumination (figure 4(a)). It can bee seen that the rise and decay of the photoresponse is slow. It is important to note that ZnO film deposited on an SS substrate is preferentially oriented along the *c*-axis and showed a reasonably good UV photoconductivity. This result is in contradiction to the earlier reported results where no appreciable photoconductivity was observed in the *c*-axis oriented sputtered ZnO films [11, 12]. The observed photoconductivity in the *c*-axis oriented films may be due to the presence of defects in the films deposited under an unbalanced magnetron configuration, which in turn is influenced by the processing conditions. In the present study, ZnO films were deposited at relatively high pressure, ∼30 mTorr, and higher O_2:Ar ratio (80:20). The higher pressure of oxygen may be attributed to the presence of native defects in the ZnO films and yield a UV photoresponse with the observed characteristics.

On the other hand, structure B having ZnO nanoneedles on the surface of ZnO film showed enhanced ultraviolet photoconductivity in comparison to structure A (figure 4(b)). The UV photoconductivity in structure B was initially found to increase rapidly, and then it became relatively slow under UV light illumination. When the UV was switched off, initially the photoconductivity decay was very sharp and then it became slow (figure 4(b)). The UV photoconductivity in ZnO is basically governed by two processes (i) surface related process and (ii) bulk related process. The surface related photoconductivity is primarily governed by the adsorption and desorption of the chemisorbed oxygen at the surface of the ZnO. The electron killing ability of the chemisorbed oxygen acts as a depletion layer.

i.e. $O_2(g) + e \rightarrow O_2^-$ (adsorbed species). Upon UV light illumination, the photogenerated holes are produced and release the captured adsorbed species, i.e. O_2^- ion, by leaving behind an electron, i.e. $O_2^- + h^+ \rightarrow O_2$ (g). In the bulk related process, some O_2 neutrals are embedded in the grain boundaries and form oxygen ions by taking up an electron. Upon UV light illumination, these species liberate electrons by capturing the photogenerated holes, and the photogenerated electrons drift in the electric field and contribute to the photoconductivity. This bulk related process is considered to be fast in comparison to the surface related process [11]. In the present case, the initial fast rise in the photocurrent of the ZnO nanoneedles (structure A) can be attributed to the electronic process, which involves the reduction in the barrier height due to the photogenerated electrons from the oxygen defects. The x-ray analysis revealed the polycrystalline nature of the nanoneedles and their growth at higher oxygen pressure, and subsequently the annealing in air (at 400 °C) may be responsible for the presence of oxygen as interstitial defects. Similarly, the initial fast decay of the photoconductivity of the ZnO nanoneedles (structure B) is very fast, as can be seen in figure 4(b). The initial fast decay may be attributed to the bulk related process. On the contrary, the photoresponse behavior of structure A, i.e. ZnO film without nanoneedles (figure 4(a)), seems to be governed by the surface related process where the chemisorbed oxygens are acting as shallow traps, thereby releasing electrons slowly under UV light illumination. It may be noted that the photoresponse transient behavior of structure A is similar to that of structure B except for the initial fast rise and fast decay components (figure 4). This indicates that the role of dispersal of nanoneedles on the surface of the ZnO film becomes significant during the initial phase of the response curve where the bulk related phenomena dominates, giving higher and fast photosensitivity. The surface related phenomena due to the chemisorbed oxygen on the surface of the ZnO film is also operating simultaneously, which becomes more apparent after a sufficiently long time when the surface related process dominates the bulk process.

3.3. Trap related photoconductivity

The observed photoresponse transient could be understood more clearly on the basis of traps that are either deep or shallow present in the forbidden gap region between the conduction and the valence band. The photoresponse curve obtained in structure B, i.e. the ZnO nanoneedles shown in figure 4(b), appears to be a clear case of non-steady-state where the establishment of equilibrium between the charge carriers available in the conduction band and the trapping levels requires a time that is expected to be much greater than the lifetime of the electron (τ_n). The trapping levels in such a case are called multiple trapping levels. If m is the density of charge carriers trapped at the multiple trapping levels M, then the electron density in the conduction band can be written as [19]

$$n = \beta k I[\gamma_n M\theta^2(1 - e^{-t/\theta}) + \gamma_n N_{cM}\theta t], \tag{1}$$

where k, β, and Y_n, are the optical absorption coefficient, true quantum yield, and coefficient of capture of electrons by traps. I is the intensity of UV light and N_{cM} is the effective density of states in the conduction band reduced to the trap level M. The parameter θ is defined by $1/\gamma_n(M + N_{cM})$, which has the dimension of time. According to equation (1), the rise in the photoresponse curve may be divided into two parts: one part for $t \ll \tau_n$, i.e. fast rise, and the second part for $t \gg \tau_n$, i.e. slow rise.

A linear and fast rise in the photoconductivity of the ZnO nanoneedles, i.e. structure B, was observed for $t < 1.56$ s. The linear fast rise observed in the case of ZnO nanoneedles indicates that the behavior is the bulk related process. It is interesting to note that no such linear rise was observed in the photoresponse behavior of the ZnO films without nanoneedles, indicating that

the enhancement in the true quantum yield is due to the presence of ZnO nanoneedles on the surface of the ZnO film. The major contribution to the quantum yield of the photogenerated charge carriers is expected from the ionized oxygen defects embedded at the boundaries of the polycrystalline ZnO nanoneedles. Under UV illumination the photogenerated holes combine with the ionized oxygen to release the captured electrons and this results in an increase in the quantum yield. It may be noted that the average diameter of the ZnO nanoneedles distributed on the surface of the ZnO film was ∼20 nm and it is expected that the UV light will penetrate the entire nanoneedle. This also confirms that quantum yield of charge carriers is a bulk generated process, which leads to a fast rise in the photoresponse curve of the ZnO nanoneedles as shown in figure 4(b). This is in agreement with the earlier finding of Zhang [11] where the bulk related process was identified to be faster. The enhancement in the quantum yield due to the presence of ZnO nanoneedles should also lead to a fast decay when switching UV light from the on to the off state, and has also been experimentally verified (figure 4(b)). For $t \ll \theta$, equation (1) reduces to

$$n_1 = \beta k I t. \tag{2}$$

It may be noted that equation (2) is independent of the trapping or the recombination. A kink in the photoresponse curve of the ZnO nanoneedles was observed at $t = \theta = 1.56$ s. This kink is attributed to the establishment of the equilibrium between the conduction band and the trapping levels. The subsequent relaxation under equilibrium conditions (between M levels and the conduction band) should reduce the slope of the photoresponse curve and a similar behavior was observed in the present study for $t < \theta$, as shown in figure 4(b). For $t \gg \theta$, the expression for the electron density in the conduction band (equation (1)) can be rewritten as

$$n = \beta k I t \frac{N_{cM}}{N_{cM} + M}. \tag{3}$$

Equation (3) represents a linear curve having a slope less than the slope of the curve represented by equation (2) by a factor $N_{cM}/(M + N_{cM})$, which is the fraction of charge carrier density available in the conduction band and the remaining charge carriers are at the trapping levels (M). Under equilibrium condition $M > 0$ and a kink with an abrupt change in the slope of the photoresponse curve is expected at $t = \theta$. If the trapping levels tend to zero (i.e. $M \to 0$), the second slope of the photoresponse curve (for $t > \theta$) tends to reach the initial slope ($t < \theta$). Therefore, we can infer that the presence of trapping levels and their density are critical and have a significant role on the photoresponse behavior. In the absence of any traps, the photocurrent produced by the UV light illumination should quickly rise, corresponding to the true quantum yield with a slope $\beta K I$, as observed in the present case of ZnO nanoneedles for $t < \theta$ (figure 4(b)). When a slow rise in the photoresponse behavior was observed (figure 4(b)) for $t > \theta$, the ratio of n to m corresponds to thermal equilibrium and in the absence of degeneracy the electron density for $t > \theta$ is given by [19]

$$n_2 = \beta k I \tau_n (1 - \mathrm{e}^{-\frac{t}{\tau'}}) \qquad \text{where } \tau' = \tau_n \left(1 + \frac{M}{N_{cM}}\right). \tag{4}$$

The equations (2) and (4) represent the charge carrier density under UV light illumination for a photoconducting sample for $t < \theta$ and $t > \theta$ respectively. The electron density in the conduction band at time t under UV light illumination can be expressed as

$$n = n_1[u(t) - u(t - \theta)] + n_2[u(t - \theta)], \tag{5}$$

where $u(t)$ is the unit step function. The observed photoresponse in the ZnO nanoneedles was qualitatively analyzed by fitting the experimental data using the theoretical equations (1)–(5). The value of $\beta K I$ and N_{cM}/M was estimated from the fitting of equations (2) and (3).

The experimentally observed photoresponse curves match very well with the theoretical curve generated using the fitting parameters. The average lifetime of the charge carriers was estimated to be ∼1.56 s for $t \leqslant \theta$, and was found to increase with increasing time ($t > \theta$) to an average value of ∼17.56 s. The increase in the average lifetime of the electrons after $t > \theta$ is due to the equilibrium between the carriers present in the conduction band and the trapping levels.

Initially ($t \leqslant \theta$) the charge carriers jump to the conduction band under UV light illumination and the role of trapping centers or the recombination centers can be eliminated in this region. Therefore, during this time the dominating mechanism for the photoconductivity is the bulk related process, which leads to lower the lifetime of the charge carriers by ruling out the possibility of interactions with the trapping levels. However, after some time ($t \approx \theta$), an equilibrium is established between the charge carriers present in the conduction band and M trapping levels. It is expected that the charge carriers, after being captured by the trapping levels, jump back to the conduction band due to the thermal transition. The process of equilibrium remains until the electron manages to meet a hole and finally recombines. Thus, the trapping phenomena ultimately result in an increase in average lifetime of the electrons from 1.56 s to 17.56 s. After $t > \theta$, the fraction of electrons present in the conduction band, i.e. $N_{cM}/(M + N_{cM})$, is estimated to be around 13% and the rest of the charge carriers remain at the M trapping levels. The return probability ($\gamma_n N_{cM}$) of the electrons to the conduction band is found to be $\sim 8 \times 10^{-2}$. The smaller value of the return probability also indicates that the probability of electrons remaining at the M levels is greater than their possible transition to the conduction band. The availability of large numbers of charge carriers at the M levels supports the earlier explained mechanism of an increase in the average lifetime of the electrons. Since the M levels are highly populated ($t > \theta$), these electrons do not take part in the photoconduction process and the rise in photocurrent (for $t > \theta$) is reduced with time by a fraction $N_{cM}/(M + N_{cM})$.

When UV light illumination was switched off, the initial decay in the photoresponse behavior of structure B (ZnO nanoneedles) was very fast followed by a slow decay (figure 4(b)). However, no such fast initial decay was observed in the photoresponse decay curve of the structure A, i.e. ZnO thin films that were without nanoneedles (figure 4(a)). The fast initial decay in the ZnO nanoneedles is attributed to the bulk related phenomena as explained earlier. The decay transient was found to follow the exponential decay after the initial fast fall, i.e. $\beta k I \tau_n e^{-t/\tau}$.

The slow photoresponse at the onset when the UV was switched on and at the removal of UV light in the structure A (ZnO films without nanoneedles) is attributed to the surface related process. Chemisorbed oxygen species on the surface of the ZnO film act as shallow trapping levels. The equilibrium is maintained between the conduction band and the shallow trapping level soon after the UV light was switched on and off. This is in contrast to the photoresponse behavior observed in structure B (ZnO films with nanoneedles), where the equilibrium is established between the photogenerated charge carriers in the conduction band and the trapping levels after a time $t \approx \theta$. The photoresponse transient behavior of structure A was also fitted theoretically using equations (2)–(5) and utilizing the same fitting parameters as obtained for structure B except $\beta K I = 0$ (eliminating the fast rise). It is interesting to note that the observed fitted curve matches well with the experimentally observed photoresponse curve of structure A. This clearly suggests that the contribution of ZnO nanoneedles is significant in enhancing the photoconductivity and the initial fast rise and fast decay. However, after $t = \theta$, the response behavior of both structures A and B became nearly similar and this is due to the surface related defects in the ZnO film (figure 4).

When tested at varying UV light intensities, the ZnO film with and without ZnO nanoneedles showed a linear variation (figure 5). However, the slope of the linear curve

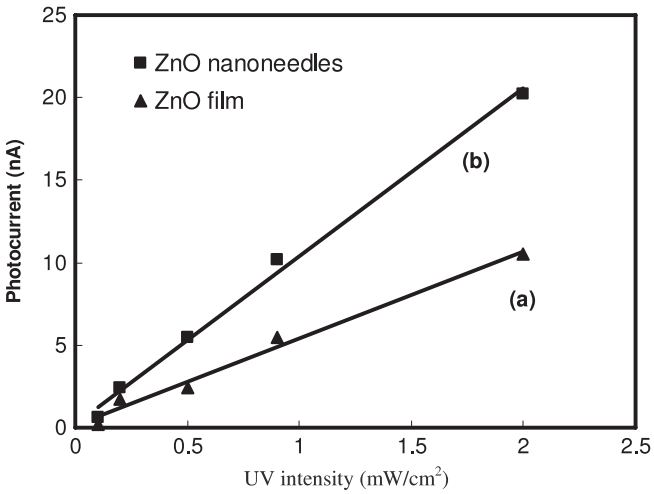

Figure 5. Variation of photocurrent with UV light intensity for: (a) ZnO film (2 μm) on an SS substrate, and (b) ZnO nanoneedles obtained on the surface of the ZnO film after annealing the ZnO multilayer at 400 °C.

corresponding to a ZnO film having nanoneedles (structure B) is more than the ZnO film without nanoneedles (structure A). The true quantum yield of a photoconducting material depends on the UV light intensity. The quantum yield in structure B is more due to the presence of nanoneedles, thereby yielding a linear curve having a higher slope in comparison to structure A (figure 5).

4. Conclusions

The presence of ZnO nanoneedles on the surface of ZnO film showed interesting photoconductivity behavior. The surface covered with the ZnO nanoneedles showed enhanced ultraviolet photoconductivity with an initial fast rise and fast decay in comparison to the ZnO films that were without nanoneedles. The fast response is attributed to the bulk related defects present in the ZnO nanoneedles, while the successive slow response is due to the establishment of equilibrium between charge carriers in the conduction band and the trapping levels due to the surface related defects in ZnO film. The enhanced UV photoconductivity in the ZnO nanoneedles could have myriad applications in designing photodetector elements with improved performance.

Acknowledgment

This work was partially supported by grant No. (R01-2006-000-10065-0) from the Basic Research Program of the Science and Engineering Foundation. SK is grateful to the BK21 for financial assistance.

References

[1] Shalish H, Temkin H and Narayanamurti V 2004 *Phys. Rev.* B **69** 245401
[2] Wang Z L 2004 *Mater. Today* **7** (June) 26–33

[3] Zhang H, Ma X, Niu J and Yang D 2003 *Nanotechnology* **14** 423
[4] Wang X, Li Q, Liu Z, Zhang J and Liu Z 2004 *Appl. Phys. Lett.* **84** 4941
[5] Huang M H, Wu Y, Feick H, Tran N, Weber E and Yang P 2001 *Adv. Mater.* **13** 113
[6] Ahn S E, Lee J S, Kim H, Kim S, Kang B H, Kim K H and Kim G T 2004 *Appl. Phys. Lett.* **84** 5022
[7] Sun Ye, Fuge G M and Ashfold M N R 2004 *Chem. Phys. Lett.* **396** 21
[8] Huang M H, Mao S, Feick H, Yan H, Wu Y, Kind H, Weber E, Russo R and Yang P 2001 *Science* **292** 1897
[9] Heo Y W, Varadarajan V, Kaufman M, Kim K, Norton D P, Ren F and Fleming P H 2002 *Appl. Phys. Lett.* **81** 3046
[10] Beermann N, Vayssieres L, Lindquist S E and Hagfeldt A 2000 *J. Electrochem. Soc.* **147** 2456
[11] Zhang D H 1995 *J. Phys. D: Appl. Phys.* **28** 1273
[12] Sharma P, Sreenivas K and Rao K V 2003 *J. Appl. Phys.* **93** 3963
[13] Kumar S, Gupta V and Sreenivas K 2005 *Nanotechnology* **16** 1167
[14] Kumar S, Sharma P and Sreenivas K 2005 *Semicond. Sci. Technol.* **20** L27
[15] Kind H, Yan H, Messer B, Law M and Yang P 2002 *Adv. Mater.* **14** 158
[16] Keem K, Kim H, Kim G-T, Lee J S, Min B, Cho K, Sung M-Y and Kim S 2004 *Appl. Phys. Lett.* **84** 4376
[17] Yao B D, Chan Y F and Wanga N 2002 *Appl. Phys. Lett.* **81** 757
[18] Wang L, Zhang X, Zhao S, Zhou G, Zhou Y and Qi J 2005 *Appl. Phys. Lett.* **86** 024108
[19] Ryvkin S M 1964 *Photoconductivity Effect in Semiconductors* (New York: Consultants Bureau) p 129